Published in final edited form as:
Free Radic Biol Med. 2012 May 1; 52(9): 1569–1576. doi:10.1016/j.freeradbiomed.2012.02.009.

Expression of lactoperoxidase in differentiated mouse colon epithelial cells

Byung-Wook Kim, **R. Steven Esworthy**, **Maria A. Hahn**, **Gerd P. Pfeifer**, and **Fong-Fong Chu***
Department of Cancer Biology, Beckman Research Institute of the City of Hope, Duarte, California 91010

Abstract

Lactoperoxidase (LPO) is known to be present in secreted fluids, such as milk and saliva. Functionally, LPO teams up with dual oxidases (DUOXs) to generate bactericidal hypothiocyanite in the presence of thiocyanate. DUOX2 is expressed in intestinal epithelium, but there is little information on LPO expression in this tissue. To fill the gap of knowledge, we have analyzed *Lpo* gene expression and its regulation in mouse intestine. In wild-type (WT) C57BL/6 (B6) mouse intestine, an appreciable level of mouse *Lpo* gene expression was detected in the colon, but not the ileum. However, in the B6 mice deficient in glutathione peroxidase (GPx)-1 and -2, GPx1/2-double knockout (DKO), which had intestinal pathology, the colon Lpo mRNA levels increased 5- to 12-fold depending on mouse age. The Lpo mRNA levels in WT and DKO 129S1/SvlmJ (129) colon were even higher, 9- and 5-fold, than B6 DKO colon. Higher levels of Lpo protein and enzymatic activity were also detected in the 129 mouse colon than B6 colon. Lpo protein was expressed in the differentiated colon epithelial cells, away from crypt base, as shown by immunohistochemistry. Similar to human LPO mRNA, mouse Lpo mRNA had multiple spliced forms, although only the full-length variant 1 (V1) was translated. Higher methylation was found in 129 than B6 strain, DKO than control colon, and older than juvenile mice. However, methylation of Lpo intragenic CpG island was not directly induced by inflammation, since dextran sulfate sodium (DSS)-induced colitis did not increase DNA methylation in B6 DKO colon. Also, Lpo DNA methylation is not correlated with gene expression.

Keywords

Glutathione peroxidase; intragenic CpG island; DNA Methylation; GPx1/2-double knockout; lactoperoxidase; dextran sulfate sodium

Introduction

Lactoperoxidase (LPO; EC 1.11.1.7) is a heme-containing glycoprotein of 78 kDa found in large quantity in secretory fluids including milk, tears, saliva and lung [1]. LPO, along with myeloperoxidase (MPO), eosinophil peroxidase (EPO), and thyroid peroxidase (TPO) are members of a mammalian peroxidase family with the prosthetic heme group covalently

*Corresponding author: Fong-Fong Chu, 1500 East Duarte Road, Duarte, CA 91010, USA. Tel: 626-359-8111 x63831, FAX: 626-930-5330, fchu@coh.org.

linked to the proteins [2]. In the presence of H_2O_2, LPO oxidizes thiocyanate (SCN^-) more efficiently than other peroxidases, whereas MPO, EPO and TPO most efficiently oxidize chloride, bromide, and iodide, respectively, to form hypo(pseudo)halides [2]. After extracellular transport, thiocyanate, even at a low concentration, can be oxidized either by peroxidases to form hypothiocyanite (OSCN−), or non-enzymatically by hypochlorite (OCl −) [3]. SCN exporters are cystic fibrosis transmembrane conductance regulator (CFTR), calcium-activated chloride channels and pendrin/Slc26A4 [4]. OSCN− is tissue-innocuous but has a broad-spectrum microbicidal and microbistatic activity [5].

For LPO to carry out innate defense requires the presence of a NADPH oxidase, which produces reactive oxygen species (ROS) and SCN, which is abundant in foods. Two NADPH oxidases, dual oxidase (DUOX)-1 and -2 produce H_2O_2 directly [4]. The LPO/DUOX system has been characterized in human trachea and bronchium, where DUOX1, DUOX2 and LPO are co-expressed on apical surface of lung epithelial cells [6, 7]. In the intestinal epithelium, only DUOX2 is expressed along with NADPH oxidase 1 (NOX1) [8, 9]. Since very little is known about LPO expression in the intestine, we intended to fill the gap of knowledge to characterize mouse *Lpo* gene expression in intestinal epithelial cells.

Interestingly, the *Lpo* gene is epigenetically regulated. We have reported that the intestinal epithelial cells isolated from C57BL/6J (B6) mice deficient in two glutathione peroxidases, GPx1 and GPx2, have aberrant global CpG island methylation pattern compared to non-DKO control ileum [10]. GPx1/2-double knockout (DKO) mice have spontaneous ileocolitis, where disease severity is strain-dependent; B6 and 129S1/SvlmJ (129) DKO have mild and severe disease, respectively [11]. Shown by CpG-island microarrays, ~250 genes, including the Lpo intragenic CpG island, in B6 DKO mice have aberrant hypermethylation [10]. About 70% of the 250 methylated genes are regulated by Polycomb proteins. It was shown recently that *LPO* gene expression is suppressed by Bmi1, a component of Polycomb repressive complex 1 (PRC1), in keratinocytes and lymphocytes [12, 13]. Bmi1 is essential for self-renewal of stem cells and is a marker for intestinal crypt stem cells [14–16]. Therefore, we examined whether *Lpo* CpG island hypermethylation is associated with gene repression in mouse intestine.

In summary, we report on strain-dependent *Lpo* gene expression in the lower GI tract. Mouse Lpo mRNA is highly elevated in B6 GPx1/2-DKO colon, whereas B6 control mice have a low level of expression. High levels of Lpo RNA are found in both DKO and control 129 mouse colon. Methylation of the intragenic CpG island of the *Lpo* gene varies with mouse strain, age and GPx status, but does not directly result from inflammation nor increase in gene expression.

Material and Methods

Mice

GPx1/2-DKO mice were generated by mating $GPx1^{tm1Ysh/tm1Ysh}$ (GPx1-KO) and $GPx2^{tm2Coh/tm2Coh}$ (GPx2-KO) mice [17]. B6 (≥N7) GPx1/2 DKO and WT mice and 129 (≥N7) DKO and non-DKO mice were maintained in ventilated cages with free access to food and water. A 129 congenic line with B6 *Gdac1* locus, 129-$Gdac1^{B6}$ mice, were generated [11]. The congenic 129-$Gdac1^{B6}$ DKO mice had milder colitis than 129 DKO mice. B6 colonies were maintained on rodent chows, LabDiet 5058 and 5043 (Purina Mills, Inc., Richmond, IN) for breeders and pups, respectively, and 129 colonies were maintained on either rodent chows or purified diets containing AIN76A micronutrients for a better survival rate [18]. The Institutional Animal Care and Use Committee approved all procedures done on mice.

Dextran sulfate sodium (DSS) treatment

Because B6 DKO mice had low colon pathology/inflammation scores, we used DSS-induced acute colitis to study Lpo DNA methylation. The short-term effect of DSS was studied in B6 DKO mice given 6 days of 1.5% DSS in drinking water beginning at 26 days of age and analyzed two days after recovery on fresh water, at 34 days of age. The long-term effect of DSS was analyzed in B6 DKO mice given 7 days of 1.5% DSS beginning at 35 days of age and analyzed after 9 weeks on fresh water at 3.5 months of age.

Cell culture and generation of Lpo stable transfectant lines

Mouse CMT-93 colon cancer cells (ATCC, Manassas, VA 20108) were maintained in DMEM/F12 medium with 10% heat-inactivated fetal bovine serum. Since these cells expressed extremely low levels of endogenous *Lpo* mRNA, we generated stable *Lpo* transfectant clones in CMT-93 cells from an open-reading frame (ORF) of *Lpo* cDNA subcloned from a full-length cDNA in pCMV6-Kan/Neo plasmid (MC201302, Origene Technologies, Inc., Rockville, MD). The forward primer contains a Kozak sequence and a *Kpn*I restriction site: 5′-CTGGATCCGGTACCGAGGAGATCTGCCGCC GCGATCGC GTGATGAAAGTGCTTCTGCAT-3′; the reverse primer has a *Hind*III site: 5′-GGGCAGA AGCTTCCTACTCCTTCACTGAGGCC-3′. The PCR product was gel-purified using a QIAquick Gel Extraction kit (Qiagen, Valencia, CA) and cloned into pCR2.1 (TA Cloning Kit, Invitrogen, Carlsbad, CA). The Lpo ORF was excised with *Kpn*I and *Hind*III from pCR2.1 to clone into pCMV6-Kan/Neo. The Lpo ORF-pCMV6-Kan/Neo was transfected into CMT-93 cells using Lipofectamine 2000 (Invitrogen) and stably transfected clones were selected with 0.4 mg/ml G418 sulfate (Research Products International Corp. Mt. Prospect, IL). Clones with higher enzymatic activity were used for Western analysis. Lpo variant 2 (V2) cDNA was subcloned with forward primer: 5′-CTGGATCCGGTACCGAGGAGATCTGCCGCCGCGATCGCAAGATGGCC ATGACAA CCAAG-3′ and the same reverse primer for the Lpo ORF clone.

Quantification of mRNA with real-time PCR (qPCR) and detection of Lpo cDNA variants

Mice were euthanized by CO_2 asphyxiation. Tissues including liver, lung, stomach, jejunum, ileum, colon and rectum (the most distal 1 cm of colon) were dissected out and stored in RNAlater (Qiagen) at −80°C. After homogenization with Polytron homogenizer (PT 1200 E, Brinkmann Kinematica, Fisher Scientific) for tissue or sonication for cell pellet, RNA was isolated with RNeasy Mini kit (Qiagen). cDNA was synthesized from 2 μg of total RNA using M-MLV reverse transcriptase (Promega, Madison, WI) and random hexamers (Invitrogen) as primers.

The Lpo primers (spanning exons 1–4) used for screening tissue expression pattern producing a 249 bp amplicon by reverse-transcribed PCR (RT-PCR) were: forward 5′-AAGGCACACTGCAGTGATGAAA-3′ and reverse 5′-TTGGCATGCTTGAGA TAATCTGAC-3′. Another Lpo primer set, spanning exons 1–7, to detect splicing variants were: forward 5′-ACCTCGCAAAATCCTTCCC-3′ and reverse 5′-GTATCACTC CCCATTTCAGTTTC-3′. Each variant form was extracted from agarose gels and sequenced (Hitachi AB Model 3730 DNA Analyzer).

A third Lpo primer set, flanking exons 9–10, for qPCR were: 5′-ACATCCCAC ACACTCTTTATC-3′ and 5′-CCACTTCTGCATCTCATCAC-3′. The primers for mouse Saa3 primers are 5′-TGCCATCATTCTTTGCATCTTGA-3′ and 5′-CCGTGAACTTCTGA ACAGCCT-3′. The mRNA levels were normalized against β-actin mRNA (5′-GCTCC TCCTGAGCGCAAGT-3′ and 5′-TCATCGTACTCCTGCTTGCTGAT-3′). All qPCRs were performed with the Eva qPCR

SuperMix kit containing SYBR Green dye (BioChain Institute, Inc. Hayward, CA) using iQ5 Detection System (Bio-Rad Labs, Hercules, CA). Each assay was done in triplicate.

Western blotting

Cells or tissue samples were homogenized in a buffer containing 10 mM Tris, pH 8.0, 1% NP-40, 150 mM NaCl, 1 mM EDTA and protease inhibitors (Protease Inhibitor Cocktail, P8340, SIGMA, St. Louis, MO) by Polytron homogenizer and followed by sonication. After centrifugation at 12,000 × *g* at 4°C, the supernatant protein was quantified with BCA assay (Pierce, Rockford, IL). After resolving 100 μg proteins in 7.5% SDS-polyacrylamide gels by electrophoresis, proteins were transferred to nitrocellulose membranes (Whatman, UK) using a semi-dry transfer apparatus (Bio-Rad). After transfer, the membrane was blocked with 5% bovine serum albumin in phosphate buffered saline with 0.1% Tween-20, pH 7.4, at room temperature for 1 h with gentle agitation. The membrane was then incubated with 1,000X diluted-rabbit polyclonal anti-LPO antibody (PA146353, Fisher Scientific) overnight at 4°C. Ab binding was detected with 2,000X diluted HRP-conjugated goat anti-rabbit IgG (Jackson ImmunoResearch Labs, West Grove, PA) for 1 h. Mouse anti-β actin Ab (A1978, Sigma) was used for normalization. The signal was detected with ECL substrate (Pierce) and chemiluminescence captured by X-ray films was quantified with QuantityOne (BioRad) software.

Immunohistochemistry

After fixing in 10% phosphate-buffered formalin overnight, tissues were dehydrated and embedded in paraffin and sectioned. The same rabbit polyclonal anti-LPO antibody for Western was used to detect Lpo protein on fixed-tissue sections. Biotinylated goat anti-rabbit IgG antibody (Vector Lab, CA) was used as second Ab and detected by streptoavidin-HRB complex (Vector laboratories, Burlingame, CA) and visualized with 3,3′-diaminobenzidine (BD Biosciences, CA). Sections were counterstained with Mayer's hematoxylin.

Peroxidase assay

Total colon or cell pellet was homogenized by Polytron or sonication in PEC buffer containing 50 mM potassium phosphate, pH 6.0, 1 mM EDTA, 0.5% cetyl-trimethylammonium bromide, and a protease inhibitor cocktail [19]. The reaction mixture contained 5 μg of proteins from supernatant, 100 mM sodium acetate, pH 5.2, 0.15 mM H_2O_2 and 0.7 mM 3.3′,5,5′-tetramethylbenzidine (TMB, Sigma) and incubated at 37°C for 3 min. After stopping reaction with 0.5 M HCl, the reaction product was measrued at A_{450}. We used 100 mM NaCl to inhibit 90% Mpo and 70% Epo activities, and 100 μM resorcinol to inhibit >90% Lpo and 70% Epo activities. A standard curve generated with 1–20 ng bLPO was used to estimate Lpo activity in the lysate.

Combined-bisulfite-restriction analysis (COBRA) of DNA methylation

Epithelial cells were isolated from colon by the everted sac method as described previously [20]. Methylation in the Lpo CpG island was detected by COBRA [21]. Mouse genomic DNA was converted with bisulfite using a Zymo Gold kit (Zymo Research). The bisulfite-treated DNA was amplified with DNA fragment-specific primers (Forward: 5′-TAGGGTATTAGGTTTATAAT-3′; Reverse: 5′-CCCTCCTCCACATCTACT-3′). PCR products were digested with *Bst*UI restriction enzyme (New England Biolabs) according to a published method [21]. To quantify the extent of DNA methylation, PCR products were resolved on 2% agarose gels. Ethidium bromide-stained DNA image was captured by Epi Chemi II UVP-Bioimaging System (Upland, CA) and analyzed with QuantityOne software (BioRad). The percentage of DNA methylation was obtained by the ratio of BstU1 digested

DNA fragments (methylated DNA) to total DNA fragments (methylated and unmethylated DNA) in the same lane.

Statistical analysis

T-test was done with the Microsoft Excel program; $P<0.05$ was considered as significant.

Results

Elevated Lpo mRNA levels in the colon of B6 and 129 GPx1/2-DKO and control mice

Very little is known about *Lpo* gene expression in the gastrointestinal tract. We used RT-PCR to survey Lpo mRNA levels in distal GI tissues of B6 GPx1/2-DKO and WT mice. Lpo mRNA was detectable only in WT colon, and DKO small and large intestine, but not in the stomach, liver and lung (Figure 1A). We then compared Lpo mRNA levels between B6 DKO and WT ileum, colon and rectum, and found that DKO mice expressed higher mRNA levels than WT mice in the corresponding tissues (Figure 1B). The Lpo mRNA level was expressed higher in the colon than in the ileum. The relative level is 0.11 in DKO ileum, 0.01 in WT ileum, 0.90 in DKO colon, 0.17 in WT colon, 1.46 in DKO rectum and 0.12 in WT rectum.

Since DKO mice have spontaneous ileocolitis, and 129 DKO mice have clear inflammation when B6 DKO mice have sub-inflammatory pathology, we tested whether 129 DKO colon had even higher *Lpo* expression than B6 DKO colon. Because 129 DKO mice have a high morbidity rate, we analyzed 22-day-old mice in this study (Figure 1C). Both 129 DKO and control mice expressed higher levels of Lpo than B6 DKO mice. The relative level is 1.3 for B6 DKO, 0.1 for B6 WT, 6.6 for 129 DKO and 12.0 for 129 control mice. However, inflammation did not further increase *Lpo* gene expression in the 129 DKO colon.

Lpo protein and activity is highly expressed in 129 DKO and control colon epithelium

We used Western blotting to quantify Lpo protein expression in DKO and control mouse colon of B6 and 129 strains (Figure 2). Since the rabbit anti-LPO Ab recognizes multiple bands, untransfected and Lpo transfectant CMT-93 cells were used as negative and positive controls (Figure 2A). Lpo was ~90 kDa, larger than the purified 75 kDa bovine milk LPO (data not shown) presumably because of retention of the leader sequence. Lpo protein level after normalization with β-actin was 4.7 to 8.2 fold higher in 129 DKO and WT colon than B6 colon; however, there was no difference between DKO and WT mice in both strains (Figure 2B).

As expected, the highest peroxidase activity in the colon was detected in 129 DKO mice (Figure 2C), since 129 DKO colon had severe inflammation with infiltrating inflammatory cells expressing Mpo or Epo. Part of the peroxidase activity was contributed by Mpo, since 129 DKO colon retained significant amount of activity in the presence of 100 μM resorcinol, which inhibits Lpo and Epo. 129 DKO and control colon had similar levels of Lpo activity, when Mpo and Epo activity was inhibited by 100 mM NaCl. B6 DKO and control mice did not have frank colitis, thus they had similar background activity.

To identify the types of cells expressing Lpo in the colon, we performed immunohistochemical (IHC) staining (Figure 3). Positive staining was detected in the epithelial cytoplasm and stronger staining was seen in cells exposed to the luminal surface, away from the crypt base. As expected, B6 WT colon had the weakest staining in a spotty fashion, when both 129 WT and DKO colon had strong straining with shorter skipping. Clearly, Lpo is expressed in intestinal epithelial cells including colonocytes and mucin-containing goblet cells.

The *Lpo* gene has multiple splice variants but only variant 1 has enzymatic activity

We analyzed *Lpo* splicing variants since human *LPO* gene has three variants when expressed in the airway epithelial cells, salivary gland and breast [22]. Using a primer set in exon 1 and 7, five *Lpo* variants were identified from B6 DKO rectum (Figure 4). Unlike human *LPO* variants, which retained exon 2 containing the putative secretory-signal peptide [22], only the ~840 bp *Lpo* variant 1 (V1) retained exon 2. The rest four variants skipped both exon 2 and 3. A similar splicing pattern of the *Lpo* gene was observed in B6 DKO mouse salivary gland and in 129 DKO and control colon (Figure 6C).

Human *LPO* variant 2 (V2) skips exon 3 to make a truncated protein, but V3 skips exon 3 and 4 still making an active enzyme [22]. We tested the protein expression of *Lpo* V1 and V2 by transfection of V1 ORF and V2 in pCMV6-Kan/Neo into CMT-93 mouse colon cancer cells. Although both V1 and V2 cDNA were transcribed in transfected clones, only Lpo V1 had protein expression and peroxidase activity (Figure 5).

Hypermethylation of intragenic CpG island of *Lpo* gene in mouse colon is associated with age, GPx status and mouse strain

In our previous array analysis, we found that the *Lpo* gene (among ~250 genes) had aberrant CpG DNA methylation in the ileal epithelium of B6 and B6;129 mixed strain DKO mice compared to WT mice [10]. Here we analyzed Lpo CpG DNA methylation in DKO and WT mice in two different ages and in two inbred strains. The *Lpo* CpG island is located in exon 6 spanning into intron 6 (Figure 4B). We found 8-month-old mice have more DNA methylation than 1-month-old in both DKO and WT mice and in both B6 and 129 strains (Figure 6A and 6B). The DKO colon had significantly more methylation than WT colon in age- and strain-matched comparison, except in 129 strain 8-month-old mice which were already highly methylated. Finally, the 129 mouse colon had significantly more DNA methylation than B6 in age- and GPx-genotype-matched comparison, except the 8-month-old DKO groups. A similar pattern of age- and GPx-genotype-dependent epigenetic changes in Lpo CpG island was also detected in B6 ileum (data not shown).

Lpo DNA methylation was not accelerated by dextran sulfate sodium (DSS)-induced colitis or directly linked to gene expression

Since DKO mice have elevated colon pathology/inflammation scores, we tested whether inflammation accelerated DNA methylation. Giving mice DSS-containing water causes acute colitis, which was evident by drastic increase in serum amyloid A-3 (Saa3) expression in the colon, which is an inflammation marker (Figure 7A), analyzed at 2 days after termination of DSS-treatment to B6 DKO mice [23]. These mice have similar levels of Lpo DNA methylation as age-matched (34-day-old) control B6 DKO mice (Figure 7B). Since Katsurano et al. showed that DSS-induced DNA methylation in WT BLAL/c colon could only be detected at 8–15 weeks after recovery from the treatment but not at 1 week post-DSS treatment [24], we also analyzed DSS-treated B6 DKO mice at 9 weeks after DSS termination. Although we observed higher Lpo DNA methylation levels in these 3.5-month-old B6 DKO mice compared to the 34-day-old mice (Figure 7B), no difference was found between the treated and control B6 DKO mice.

We also correlated Lpo DNA methylation with inflammation (without DSS treatment) by comparing DNA methylation levels between 129 DKO colon and a congenic 129-Gdac1^{B6} DKO colon, which had milder colitis [11] to remove the strain, GPx status, and age variables. Again, the fact that the 129 DKO colon had a higher Saa3 mRNA levels, an inflammation marker, than the congenic 129-Gdac1^{B6} DKO colon supports its higher inflammation levels in the 129 DKO colon (Figure 7C). Since the 30-day-old 129 DKO and

129-Gdac1^{B6} DKO colon had the same level of Lpo DNA methylation, this result does not support the notion that inflammation accelerate DNA methylation (Figure 7D).

We then tested whether Lpo DNA methylation is associated with gene expression. When compared across GPx genotypes and mouse strains, hypermethylation of the *Lpo* intragenic CpG island appeared to be associated with higher gene expression. B6 DKO colon had 5- to 13-fold higher Lpo mRNA than B6 WT colon, and 129 colon has 5- to 9-fold higher Lpo mRNA levels than B6 DKO (Figure 1B and 1C). However, there was no correlation to DNA methylation when we compared Lpo mRNA levels at different ages within the same strain and DKO status. In fact, the 3.5-month-old B6 DKO control mice had significantly lower Lpo mRNA levels (0.5 ± 0.4, n=4) than 34-day-old B6 DKO control mice (1.2 ± 0.5, n=5; $P<0.05$), whereas the 3.5-month-old DKO mice had 3.4-fold higher Lpo DNA methylation than the 34-day-old mice. No difference in Lpo mRNA levels were found between 34-day-old DSS treated (0.80 ± 0.45, n=3) and control B6 DKO mice. This result does not support the notion that intragenic DNA methylation promotes gene expression.

Discussion

Very little is known about *Lpo* gene expression in the intestine. Although Lpo mRNA was detected in rat rectum [6], there has been no indication of protein expression in this tissue. In this manuscript, we have provided evidence for *Lpo* gene expression in intestinal epithelium at both the mRNA and protein levels. Mouse colon appears to express much higher Lpo than the lung, which did not have detectable mRNA. Although human LPO mRNA was detected in trachea and bronchial epithelial cells [6, 22], detection of LPO protein in respiratory tissues requires concentrating a large volume [7, 22, 25]. Mouse colon Lpo protein can be detected without concentration.

Although LPO was originally recognized as a secretory protein, well known in milk and saliva, its expression in respiratory epithelial cells, lymphocytes and keratinocytes suggest it may also have cellular functions. In trachea, LPO is expressed in serous submucosal cells, but not mucus-secreting cells, as well as in airway surface epithelial cells [22]. We found that Lpo is expressed in differentiated absorptive as well as goblet cells but not in the mucin-containing granules. Since Duox2 is also expressed in surface colon epithelium [8], and Duox/Tpo complex has been observed in thyrocytes [26], it is possible that Lpo also forms complex with Duox2 for more efficient consumption of H_2O_2.

We found that increased Lpo DNA methylation correlates with aging, GPx status and mouse strain. Age-dependent changes in DNA methylation have been observed in both humans and mice, with more genes hypermethylated than hypomethylated [27–29]. Here, we have identified Lpo gene to be hypermethylated through aging, mostly from juvenile to adult phase. Unexpectedly, the GPx1/2-DKO-associated hypermethylation may not be driven by inflammation, since DSS-treatment did not accelerate Lpo DNA methylation in B6 DKO colon, and similar levels of methylation were found between 129 DKO and its congenic 129-Gdac1^{B6} DKO mouse colon, which had milder colitis. DSS-accelerated DNA methylation has been reported in BALB/c colon on *Fosb, Msx1* and *Sox11* CpG identified by microarray analysis of methylated DNA [24]. However, this epigenetic change is likely associated with carcinogenesis process since significant increases in these three CpG islands are detected at 15 weeks after cessation of DSS treatment, and 2 of six DSS-treated BALB/c mice had colon tumor. Another case of inflammation-associated aberrant DNA methylation was described in *Helicobacter pylori*-infected gastric epithelium of Mongolian gerbils [30]. Because the gerbils were pretreated with MNU mutagen and no significant methylation changes were detected until 10–50 weeks post-infection, the epigenetic changes are most likely associated with carcinogenesis rather than resulting from inflammation.

Our study suggests that inflammation per se does not accelerate Lpo DNA hypermethylation in mouse colon. Because DKO intestinal epithelial cells have higher rate of proliferation and apoptosis than WT mice in both B6 and 129 strains [31](and unpublished observation), it is possible that faster cell turnover accelerates DNA methylation, similar to aging. On the other hand, the strain-dependent epigenetic changes are not well understood. Here, we have provided an example of the strain-dependent DNA methylation.

Whether methylation in the intragenic CpG island is associated with gene expression or not is not well understood. When we compared DNA methylation across GPx genotypes and mouse strains, hypermethylation of the *Lpo* intragenic CpG island appeared to be associated with higher gene expression. However, when we correlated gene expression and DNA methylation levels within the same strain and GPx status mice, the hypermethylated Lpo DNA appeared to have lower gene expression. Therefore, it is unclear whether Lpo methylation has a direct impact on gene expression. Although hypermethylated promoter CpG islands are associated with gene silencing, several correlative studies suggest that hypermethylation of the intragenic CpG island is linked to gene activation. Hellman and Chess showed that the active human X chromosome displays more than two-fold higher methylation at gene bodies than the inactive X [32]. Murrell et al. showed that an intragenic methylated region in the paternally imprinted Igf2 gene augmented transcription [33]. Rauch et al. have shown that genome-wide gene-body hypermethylation is in conjunction with elevated transcription levels [34]. Recently, Lai et al. showed that hypermethylation of the intragenic CpG island in human *BCL6* oncogene promoted *BCL6* transcription during lymphomagenesis [35]. More experimental studies should be conducted to determine whether one can reach a consensus on the consequence of hypermethylation in gene bodies.

A physiological function of Lpo in the intestinal mucosa is to produce hypothio-cyanite ion by coupling with H_2O_2-generating NADPH oxidases [4]. Co-regulation of Lpo and NADPH oxidase gene expression has been reported in several tissues. In thymocytes, Bmi1 represses *Lpo, Duox1* and *Duox2* expression [13], while in keratinocytes, BMI1 represses *LPO, NOX1, NOXO1, NOX4, NOXO2*, but not *DUOX1* or *DUOX2* expression induced by irradiation [12]. Since Lpo and Bmi1 is expressed in mature and crypt stem epithelial cells, respectively, in the colon [14] [15, 16], other factors may be involved in *Lpo* gene activation. We need to explore how the Lpo gene expression is regulated in the colon. Once identified, we will use the regulators to modulate Lpo gene expression and to determine whether Lpo is coregulated with Nox1 or Duox2, two major NADPH oxidases, in intestinal epithelium. It is possible that co-localization of Lpo and Nox1 or Duox2 is sufficient to fend off bacteria invasion without co-regulation of gene expression.

The Lpo gene has multiple splice variants, but apparently only the predominant full-length V1 has enzymatic activity. All other variants skip exon 2, which has a leader sequence, and exon 3. These variants without the leader sequence are unlikely to be translated, because a) the Lpo V2 is not translated, and V3-V5 miss more exons than V2; and b) the N-terminal amino acid of various LPO preparations has exon 3 peptide [36]. Thus, the physiological significance of *Lpo* splice variants is unknown.

Conclusions

Mouse *Lpo* gene is highly expressed in the distal intestine, and in the mature epithelial cells away from the crypt stem cells. The colon *Lpo* gene is epigenetically regulated at its intragenic CpG island, its methylation level varies depending on mouse strain, age and GPx status. Hypermethylation of the Lpo DNA is not directly linked to inflammation or increase in gene expression.

Acknowledgments

The authors thank Sofia Loera and Tina Montgomery of the Anatomic Pathology Core for tissue processing and Hector Rivera in the DNA Sequencing Core. *Grant support*- Part of this work was supported by National Institutes of Health grants (R01 CA114569 and P30 CA033572).

Abbreviations

129	129S1/SvlmJ
B6	C57BL/6J
Bmi1	B lymphoma Mo-MLV insertion region 1
COBRA	combined-bisulfite-restriction analysis
DKO	double knockout
Duox	dual oxidase
EPO	eosinophil peroxidase
GPx	glutathione peroxidase
Lpo	lactoperoxidase
MPO	myeloperoxidase
Nox	NADPH oxidase
ORF	open-reading frame
qPCR	quantitative real-time polymerase chain reaction
RT-PCR	reverse-transcribed PCR
TPO	thyroid peroxidase
V1	variant 1
V2	variant 2

References

1. Ihalin R, Loimaranta V, Tenovuo J. Origin, structure, and biological activities of peroxidases in human saliva. Arch Biochem Biophys. 2006; 445:261–268. [PubMed: 16111647]
2. Sheikh IA, Singh AK, Singh N, Sinha M, Singh SB, Bhushan A, Kaur P, Srinivasan A, Sharma S, Singh TP. Structural evidence of substrate specificity in mammalian peroxidases: structure of the thiocyanate complex with lactoperoxidase and its interactions at 2.4 A resolution. J Biol Chem. 2009; 284:14849–14856. [PubMed: 19339248]
3. Xu Y, Szep S, Lu Z. The antioxidant role of thiocyanate in the pathogenesis of cystic fibrosis and other inflammation-related diseases. Proc Natl Acad Sci U S A. 2009; 106:20515–20519. [PubMed: 19918082]
4. Rada B, Leto TL. Oxidative innate immune defenses by Nox/Duox family NADPH oxidases. Contrib Microbiol. 2008; 15:164–187. [PubMed: 18511861]
5. Rada B, Leto TL. Redox warfare between airway epithelial cells and Pseudomonas: dual oxidase versus pyocyanin. Immunol Res. 2009; 43:198–209. [PubMed: 18979077]
6. Geiszt M, Witta J, Baffi J, Lekstrom K, Leto TL. Dual oxidases represent novel hydrogen peroxide sources supporting mucosal surface host defense. FASEB J. 2003; 17:1502–1504. [PubMed: 12824283]
7. Gattas MV, Forteza R, Fragoso MA, Fregien N, Salas P, Salathe M, Conner GE. Oxidative epithelial host defense is regulated by infectious and inflammatory stimuli. Free Radic Biol Med. 2009; 47:1450–1458. [PubMed: 19703552]

8. El Hassani RA, Benfares N, Caillou B, Talbot M, Sabourin JC, Belotte V, Morand S, Gnidehou S, Agnandji D, Ohayon R, Kaniewski J, Noel-Hudson MS, Bidart JM, Schlumberger M, Virion A, Dupuy C. Dual oxidase2 is expressed all along the digestive tract. Am J Physiol Gastrointest Liver Physiol. 2005; 288:G933–942. [PubMed: 15591162]
9. Kuwano Y, Kawahara T, Yamamoto H, Teshima-Kondo S, Tominaga K, Masuda K, Kishi K, Morita K, Rokutan K. Interferon-gamma activates transcription of NADPH oxidase 1 gene and upregulates production of superoxide anion by human large intestinal epithelial cells. Am J Physiol Cell Physiol. 2006; 290:C433–443. [PubMed: 16162660]
10. Hahn MA, Hahn T, Lee DH, Esworthy RS, Kim BW, Riggs AD, Chu FF, Pfeifer GP. Methylation of polycomb target genes in intestinal cancer is mediated by inflammation. Cancer Res. 2008; 68:10280–10289. [PubMed: 19074896]
11. Esworthy RS, Kim BW, Larson GP, Yip ML, Smith DD, Li M, Chu FF. Colitis locus on chromosome 2 impacting the severity of early-onset disease in mice deficient in GPX1 and GPX2. Inflamm Bowel Dis. 2011; 17:1373–1386. [PubMed: 20872835]
12. Dong Q, Oh JE, Chen W, Kim R, Kim RH, Shin KH, McBride WH, Park NH, Kang MK. Radioprotective effects of bmi-1 involve epigenetic silencing of oxidase genes and enhanced DNA repair in normal human keratinocytes. J Invest Dermatol. 2011; 131:1216–1225. [PubMed: 21307872]
13. Liu J, Cao L, Chen J, Song S, Lee IH, Quijano C, Liu H, Keyvanfar K, Chen H, Cao LY, Ahn BH, Kumar NG, Rovira, Xu XL, van Lohuizen M, Motoyama N, Deng CX, Finkel T. Bmi1 regulates mitochondrial function and the DNA damage response pathway. Nature. 2009; 459:387–392. [PubMed: 19404261]
14. Park IK, Morrison SJ, Clarke MF. Bmi1, stem cells, and senescence regulation. J Clin Invest. 2004; 113:175–179. [PubMed: 14722607]
15. Sanchez-Beato M, Sanchez E, Gonzalez-Carrero J, Morente M, Diez A, Sanchez-Verde L, Martin MC, Cigudosa JC, Vidal M, Piris MA. Variability in the expression of polycomb proteins in different normal and tumoral tissues. A pilot study using tissue microarrays. Mod Pathol. 2006; 19:684–694. [PubMed: 16528373]
16. Abdul Khalek FJ, Gallicano GI, Mishra L. Colon cancer stem cells. Gastrointest Cancer Res. 2010:S16–23. [PubMed: 21472043]
17. Esworthy RS, Aranda R, Martin MG, Doroshow JH, Binder SW, Chu FF. Mice with combined disruption of Gpx1 and Gpx2 genes have colitis. Am J Physiol Gastrointest Liver Physiol. 2001; 281:G848–855. [PubMed: 11518697]
18. Esworthy RS, Smith DD, Chu FF. A Strong Impact of Genetic Background on Gut Microflora in Mice. Int J Inflam. 2010; 2010:986046. [PubMed: 20976020]
19. Grisham MB, Benoit JN, Granger DN. Assessment of leukocyte involvement during ischemia and reperfusion of intestine. Methods Enzymol. 1990; 186:729–742. [PubMed: 2172726]
20. Esworthy RS, Swiderek KM, Ho YS, Chu FF. Selenium-dependent glutathione peroxidase-GI is a major glutathione peroxidase activity in the mucosal epithelium of rodent intestine. Biochim Biophys Acta. 1998; 1381:213–226. [PubMed: 9685647]
21. Xiong Z, Laird PW. COBRA: a sensitive and quantitative DNA methylation assay. Nucleic Acids Res. 1997; 25:2532–2534. [PubMed: 9171110]
22. Fragoso MA, Torbati A, Fregien N, Conner GE. Molecular heterogeneity and alternative splicing of human lactoperoxidase. Arch Biochem Biophys. 2009; 482:52–57. [PubMed: 19059195]
23. Gao Q, Esworthy RS, Kim BW, Synold TW, Smith DD, Chu FF. Atherogenic diets exacerbate colitis in mice deficient in glutathione peroxidase. Inflamm Bowel Dis. 2010; 16:2043–2054. [PubMed: 20848490]
24. Katsurano M, Niwa T, Yasui Y, Shigematsu Y, Yamashita S, Takeshima H, Lee MS, Kim YJ, Tanaka T, Ushijima T. Early-stage formation of an epigenetic field defect in a mouse colitis model, and non-essential roles of T- and B-cells in DNA methylation induction. Oncogene. 2011
25. Wijkstrom-Frei C, El-Chemaly S, Ali-Rachedi R, Gerson C, Cobas MA, Forteza R, Salathe M, Conner GE. Lactoperoxidase and human airway host defense. American Journal of Respiratory Cell & Molecular Biology. 2003; 29:206–212. [PubMed: 12626341]

26. Song Y, Ruf J, Lothaire P, Dequanter D, Andry G, Willemse E, Dumont JE, Van Sande J, De Deken X. Association of duoxes with thyroid peroxidase and its regulation in thyrocytes. J Clin Endocrinol Metab. 2010; 95:375–382. [PubMed: 19952225]
27. Maegawa S, Hinkal G, Kim HS, Shen L, Zhang L, Zhang J, Zhang N, Liang S, Donehower LA, Issa JP. Widespread and tissue specific age-related DNA methylation changes in mice. Genome Res. 2010; 20:332–340. [PubMed: 20107151]
28. Kellermayer R, Balasa A, Zhang W, Lee S, Mirza S, Chakravarty A, Szigeti R, Laritsky E, Tatevian N, Smith CW, Shen L, Waterland RA. Epigenetic maturation in colonic mucosa continues beyond infancy in mice. Hum Mol Genet. 2010; 19:2168–2176. [PubMed: 20197410]
29. Takasugi M. Progressive age-dependent DNA methylation changes start before adulthood in mouse tissues. Mech Ageing Dev. 2011; 132:65–71. [PubMed: 21184773]
30. Niwa T, Tsukamoto T, Toyoda T, Mori A, Tanaka H, Maekita T, Ichinose M, Tatematsu M, Ushijima T. Inflammatory processes triggered by Helicobacter pylori infection cause aberrant DNA methylation in gastric epithelial cells. Cancer Res. 2010; 70:1430–1440. [PubMed: 20124475]
31. Lee DH, Esworthy RS, Chu C, Pfeifer GP, Chu FF. Mutation accumulation in the intestine and colon of mice deficient in two intracellular glutathione peroxidases. Cancer Res. 2006; 66:9845–9851. [PubMed: 17047045]
32. Hellman A, Chess A. Gene body-specific methylation on the active X chromosome. Science. 2007; 315:1141–1143. [PubMed: 17322062]
33. Murrell A, Heeson S, Bowden L, Constancia M, Dean W, Kelsey G, Reik W. An intragenic methylated region in the imprinted Igf2 gene augments transcription. EMBO Rep. 2001; 2:1101–1106. [PubMed: 11743023]
34. Rauch TA, Wu X, Zhong X, Riggs AD, Pfeifer GP. A human B cell methylome at 100-base pair resolution. Proc Natl Acad Sci U S A. 2009; 106:671–678. [PubMed: 19139413]
35. Lai AY, Fatemi M, Dhasarathy A, Malone C, Sobol SE, Geigerman C, Jaye DL, Mav D, Shah R, Li L, Wade PA. DNA methylation prevents CTCF-mediated silencing of the oncogene BCL6 in B cell lymphomas. J Exp Med. 2010; 207:1939–1950. [PubMed: 20733034]
36. Watanabe S, Murata S, Kumura H, Nakamura S, Bollen A, Moguilevsky N, Shimazaki K. Bovine lactoperoxidase and its recombinant: comparison of structure and some biochemical properties. Biochem Biophys Res Commun. 2000; 274:756–761. [PubMed: 10924350]

Highlights

- GPx1/2-DKO mice are prone to ileocolitis in a strain-dependent manner.
- 129 strain mice have higher Lpo gene expression than B6 in the colon epithelium.
- More methylation in *Lpo* DNA is in 129 than B6, DKO than WT, mature than young mice.
- Lpo DNA methylation does not result from inflammation nor leads to gene expression.
- Only the full-length variant of colon *Lpo* mRNA produces an active enzyme.

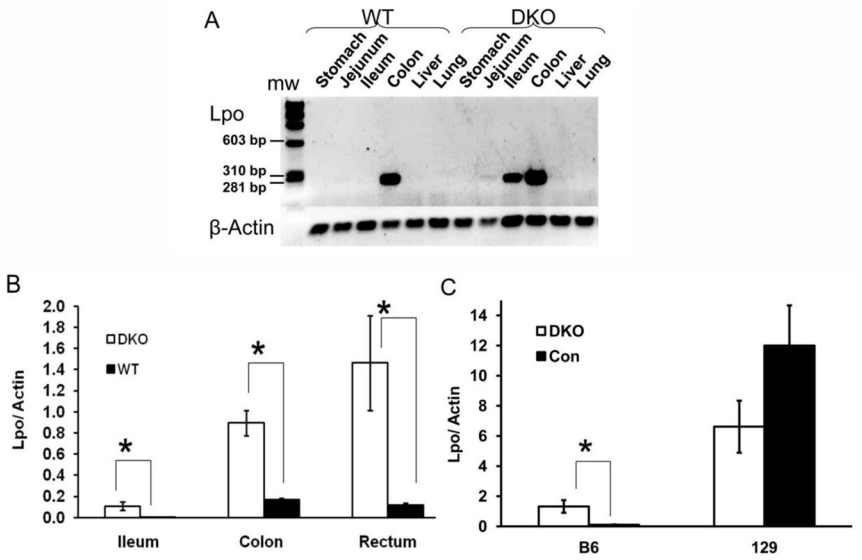

Figure 1. Expression of Lpo mRNA in mouse tissues isolated from B6 and 129 GPx-DKO and control mice

Panel A shows the detection of mRNA in stomach, jejunum, ileum, colon, liver and lung from an 8-month-old B6 wild-type (WT) and a GPx1/2-DKO mice by RT-PCR. The molecular weight (MW) marker is from *Hae*III restricted ΦX174 DNA. **Panel B** shows the relative Lpo mRNA levels in four each 30-day-old B6 DKO and WT mice in the ileum, colon and rectum. **Panel C** compares colon Lpo mRNA levels between four each 30-day-old B6 DKO and WT (the same samples as in Panel B) and five each 22-day-old 129 DKO and heterozygous control (Con) mice. Arrow bars are standard errors of means (SEM). The asterisk sign indicates significant difference between DKO and WT mice, $P<0.05$.

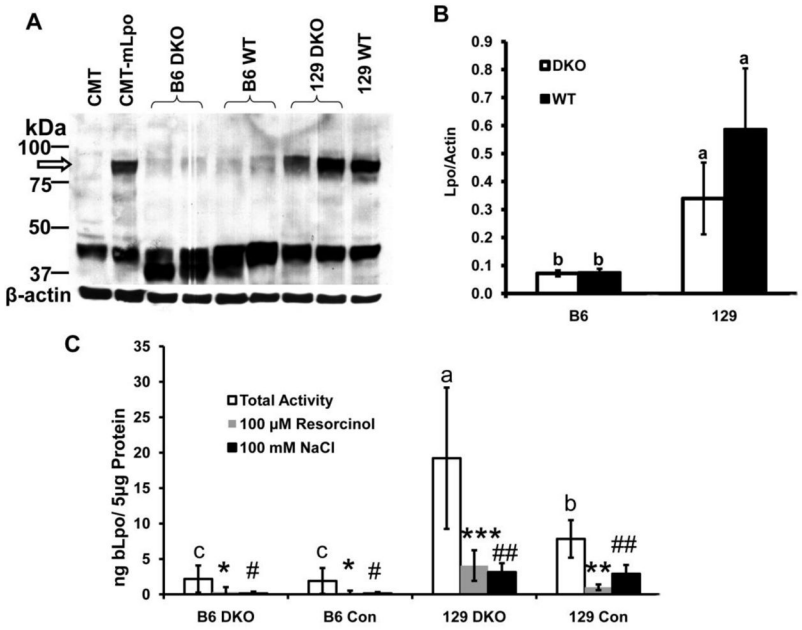

Figure 2. Lpo protein expression detected by Western blotting and activity assay

Panel A shows a Western blot of CMT-93 (CMT) cells, a CMT transfectant clone expressing Lpo ORF cDNA, colon of B6 DKO, B6 WT, 129 DKO and 129 WT 22-day-old mice, in this order. The upper panel shows the proteins recognized by anti-LPO antibody, and the lower panel shows β-actin. The open arrow points to ~90 kDa Lpo. **Panel B** shows the relative levels of Lpo protein in B6 and 129 DKO and WT colons, quantified from Western blots. Arrow bars are SEM from 4 colons in each group. Means that differ are shown with different letter, where a>b. **Panel C** shows the peroxidase activity in the colon of 10 B6 and five 129 DKO as well as 10 B6 and six 129 non-DKO control (Con) mice with at least 2 WT GPx alleles. The mean of total activity (open column) that differs is shown with different letter, where a>b>c. The mean of resorcinol-resistant activity (shaded column) that differs is shown with different number of asterisk, where ***>**>*. The mean of NaCl-resistant activity (solid column) that differs is shown with different number of number sign, where ##>#. The error bars are standard deviations of the means.

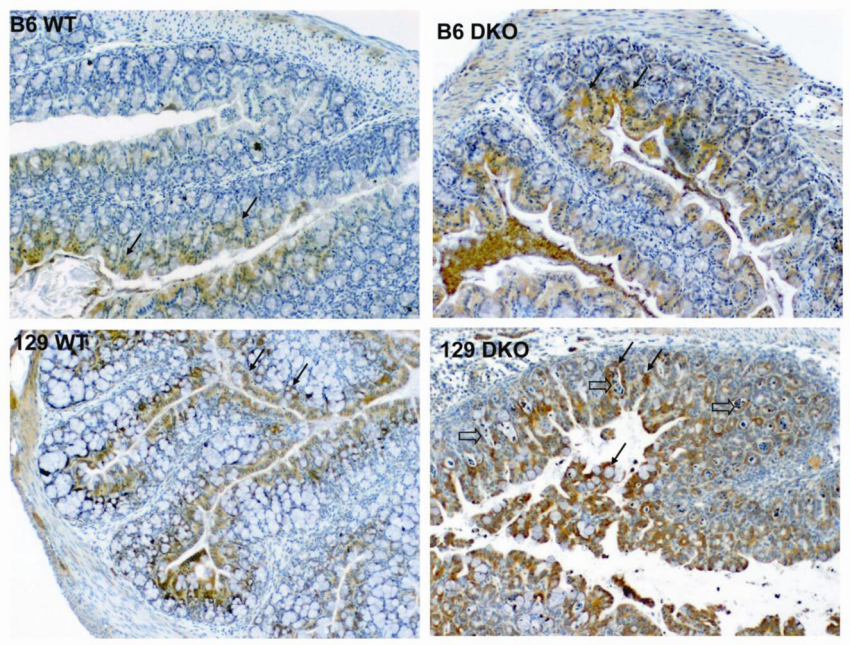

Figure 3. Immunohistochemistry of Lpo expression in colon epithelium

Cross sections of B6 WT and DKO colon as well as 129 WT and DKO colon were immunohistochemically stained with anti-LPO antibody and visualized with brown-colored DAB staining (black arrows). 129 DKO colon has many abscessed crypts (open arrows) and diminished number of goblet cells. Stronger staining is located towards surface epithelium.

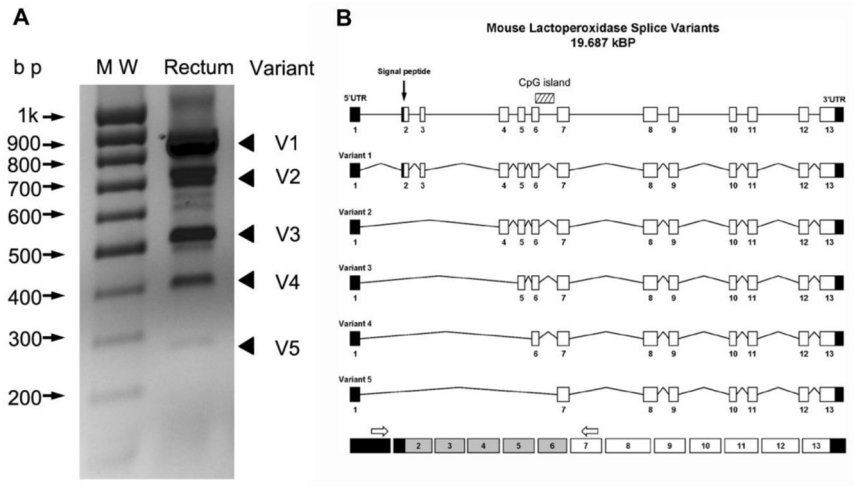

Figure 4. Splicing variants of *Lpo* gene expressed in the rectum

Panel A shows five variants (V1–V5) produced from RT-PCR of B6 DKO rectal mRNA using primers spanning exons 1 to 7 (open arrows in Panel B). Additional minor bands may come from heteroduplexes of the variants. **Panel B** is a diagram of *Lpo* gene structure and the structure of the five splice variants. Each box represents one exon, and exon 2 has a translation start site and predicted secretory signal peptide (black arrow). An intragenic CpG island is present in exon 6 and intron 6 (hatched box). The variant exons are shown as shaded boxes in the bottom diagram.

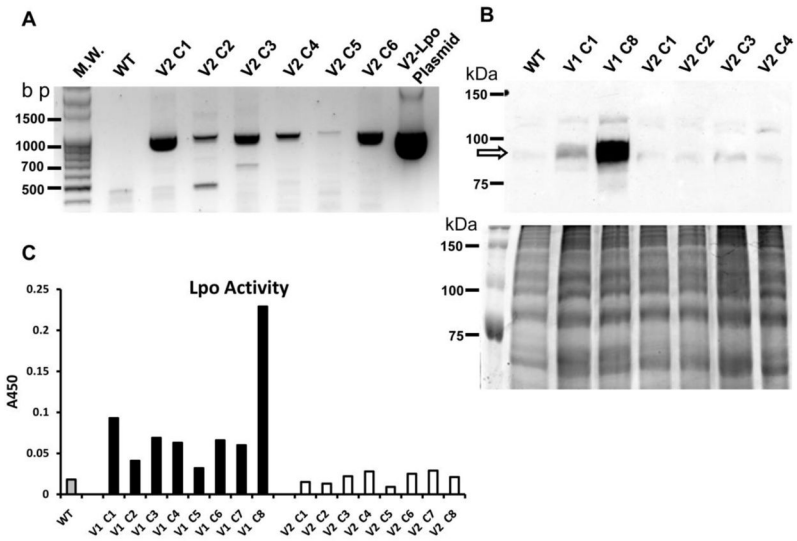

Figure 5. Lpo variant 1, but not variant 2, transfectant has protein expression and activity

Lpo variant 1 and 2 (V1 and V2) cDNAs were transfected into CMT-93 cells and stable clones (C1–C8) were isolated. Several different clones of V1 and V2 were analyzed for protein expression in Panel B and enzyme activity in Panel C. **Panel A** shows mRNA expression using primers located in exon 5 and 9. WT is un-transfected CMT-93 cells. **Panel B** illustrates a Western blot showing Lpo protein (pointed by an open arrow) detected by anti-LPO antibody (upper panel) and Coomassie blue-stained proteins for loading control in a duplicated gel (lower panel). **Panel C** shows relative peroxidase activity assayed with 5 μg cytosol using TMB substrate.

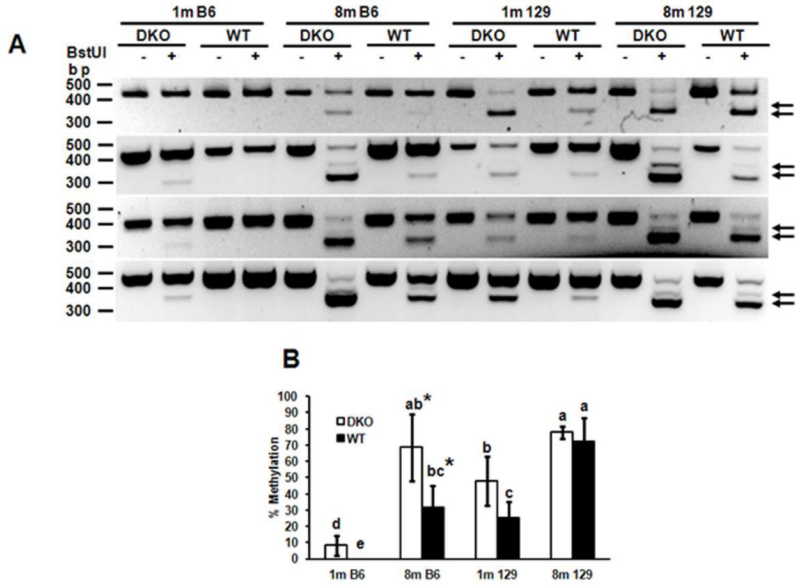

Figure 6. Different *Lpo* CpG methylation pattern and *Lpo* gene expression in the colon of B6 and 129 DKO and WT mice

Panel A shows *Lpo* CpG-island methylation analyzed by COBRA. Four colon samples were processed in each group. B6 and 129 DKO and WT mice of one month (1m) and 8 months (8m) of age were analyzed. Arrows point to the methylated DNA. **Panel B** is quantification of DNA methylation shown in Panel A. Error bars are stdev of means. The means that differ are shown with different letter, where a>b>c>d>e. The group with ab means it is not different from the groups a or b, and the group with bc means it is not different from b or c. The asterisk signs mean that ab is different from bc.

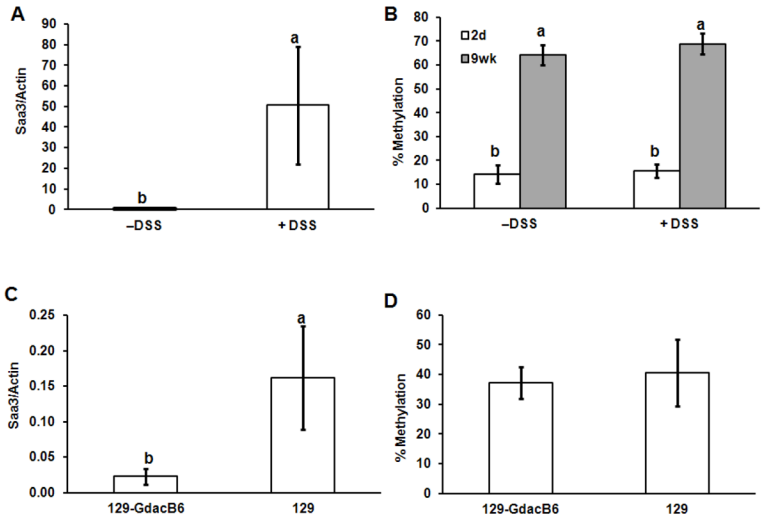

Figure 7. No correlation between colitis and DNA methylation in B6 and 129 GPx1/2-DKO mice

Panel A shows a 500-fold elevation of Saa3 mRNA level in 34-day-old B6 DKO mouse colon at 2 days after DSS termination. Five each of DSS-treated and control B6 GPx1/2-DKO mice were analyzed. Panel B shows the extent of Lpo DNA methylation in the same groups of mice studied in panel A (2d) in addition to 3.5-month-old B6 DKO mice with and without DSS treatment. Three mice were treated DSS and analyzed at 9 weeks after stopping DSS (9 wk), and 4 mice were age-matched B6 DKO control. Panel C shows 7-fold higher Saa3 mRNA levels in the colon of 129 DKO (n=3) than the congenic 129-Gdac1^{B6} DKO (n=4) mice. Panel D shows Lpo DNA methylation levels in the same mice studied in Panel C. Error bars are stdev of means. The means that differ are shown with different letter, where a>b.